JOURNAL OF OPTOELECTRONICS AND ADVANCED MATERIALS Vol. 12, No. 3, March 2010, p. 758 - 761

Combination of laser-based micro-processing and micro-analysis by means of a lensed optical fiber

S. YAKUNIN, T. STEHRER, J. D. PEDARNIG, J. HEITZ*
Institute of Applied Physics and Christian Doppler Laboratory for Laser-Assisted Diagnostics, Johannes Kepler University Linz, A-4040 Linz, Austria

We describe a scanning optical near-field microscopic (SNOM) setup allowing to produce micro-patterns by ablation, to perform laser-induced breakdown spectroscopy (LIBS), and atomic force microscope (AFM) investigation with the same optical fiber tip. The use of lensed fibers combines the advantages of high numerical aperture optics with high transmission for ns laser pulses. This allows to ignite a plasma for LIBS spectra at a certain distance between sample surface and fiber tip for increased tip durability. The tip is characterized by deconvolution from AFM measurements or by a scanned pinhole for measurement of the near- and far-field light intensity distribution.

(Received June 20, 2009; accepted October 14, 2009)

Keywords: SNOM, AFM, LIBS, Lensed fiber tips, Near-field light intensity distribution

1. Introduction

Laser micro-and nano-processing is a field of increasing practical relevance [1] . In our previous papers [2-5], we demonstrated that the combination of laser processing and SNOM technique can be used for the realization of laser-induced chemical reactions on a nanoscale, for laser ablation near the fiber tip, and for laser-induced breakdown spectroscopic (LIBS) micro-analysis of solid surface samples. As in a scanning near-field microscope (SNOM), we control the distance between a fiber tip and the sample surface by means of a shear-force sensor. We couple the laser radiation into an uncoated optical glass fiber, which had been tapered by wet chemical etching employing hydrofluoric acid as in [6] . Similar as in [7] , the tapered fiber is not glued but in close mechanical contact to the quartz tuning fork acting as the shear-force sensor.

For micro-LIBS analysis with ns laser pulses, we obtained a minimum lateral resolution of about 2 μm, which is similar to that reported by other groups for near-field and far-field experiments [8-10] . The spatial resolution limit is probably related either to insufficient sensitivity of the detection system or due to the effect that at low laser energies the hole or crater formation is based mainly on thermal processes without strong plasma formation. Another problem is the interaction of the approached tip with the plasma plume, which can result in significant etching of the tip. Therefore we employ in this work lensed optical fiber tips with higher transmission efficiency and good focusing, which also allow to perform LIBS measurements with a certain distance between sample surface and the tip for increased tip durability.

2. Experimental

Fig. 1 shows the experimental setup of a 3D scanning system with shear-force resonance sensor for tip-sample distance control in z direction. The main operation regimes of the setup are (a) AFM surface characterization, where the fiber tip is used as AFM probe, (b) micro- and submicron-processing typically with plasma formation by pulsed laser light coupled into the fiber, (c) recording of the spectral signal from the area under the tip collected and transferred to the spectrometer by a second optical fiber, and (d) investigation of the intensity distribution in front of the fiber tip by means of a scanning pin hole.

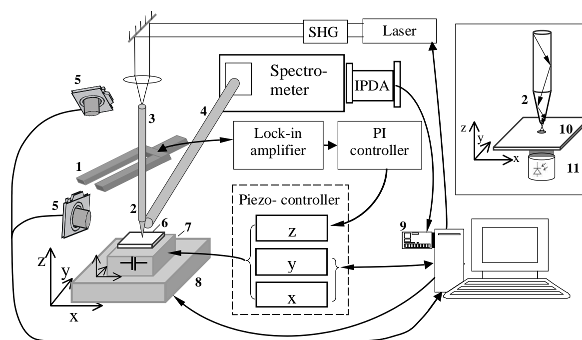

Fig. 1. SNOM-like setup for laser submicron processing and recording plasma emission spectra. The inset shows schematically the intensity distribution measurement in near- and far-field.

The setup consists of a Q-switched Nd:YAG laser with second harmonic generator (SHG), wavelength λ = 532 nm, and pulse duration of 6 ns, a glass lens with a focal length f of 70 mm coupling the laser beam to the

delivery fiber (3) that ends with the tip (2), an AFM closed-loop distance controller with quartz tuning fork (1), lock-in amplifier and proportional-integral (PI) controller, and a xyz positioning system with piezo-drives (7) and step-motor (8). The spectral recording system consists of a collection fiber (4) connected to a grating spectrometer equipped with an intensified photodiode array (IPDA), which sends the measured signals to the interface card at the computer (9). The setup includes also two digital microscopes (5) for sample observation allowing a rough determination of the position of sample and tip. A detailed description of the setup is given in [5] .

For tip shape characterization, the sample (6) can be replaced by (a) a photodiode (11) with pinhole (10) for the measurement of the intensity distribution or (b) an etalon grid. The same setup is also employed for a special grinding/polishing process to produce tips of various shapes with high optical quality and small curvature radii of a few micrometers. The details of the polishing process will be described separately in a forthcoming publication and in a pending patent [11].

3. Results and discussion

Fig. 2 shows optical microscope images of an etched sharp fiber tip and two additionally grinded fibers with spherical and conical tip shape, respectively.

Image blurring due to the finite probe size is a known disadvantage of the AFM technique. It can be described as convolution of the real image of the surface topography with the probe profile. For a single point of contact between probe and sample surface, the problem is mathematically well defined [12] and it is possible to reconstruct the real image via a deconvolution process. This can be used in a reverse way for the reconstruction of the tip shape by measurement of the known topography of an etalon grid [13].

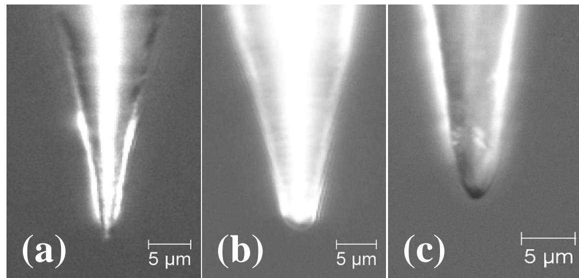

Fig. 2. Optical microscope images of (a) sharp chemically etched fiber tip and (b) spherically and (c) conically polished tips.

The AFM standard etalon Veeco SHSPT-200-CP is used as test sample for deconvolution experiments. The etalon consists of identical square holes with sharp edges. The depth of the 5x5 µm square holes is 200 nm. Fig. 3 shows the topography profile of one hole of the etalon recorded by our setup in AFM mode with a sharp etched tip and a spherical grinded tip, respectively. The nominal hole shape is also indicated in the figure.

In the case of a rectangular profile of the etalon holes, the deconvolution process simplifies and can be performed by combining the wings of the profile drooping to the bottom of the square hole (schematically indicated by the arrows a and b in Fig. 3 and Fig. 4). The result of the tip shape reconstruction is presented on Fig. 4. The experimental data properly fit with a fiber tip with the spherical shape and a radius r of about 2.8 µm. The step-height of the etalon limits the analyzed area of the tip to a 200 nm distance from the tip end.

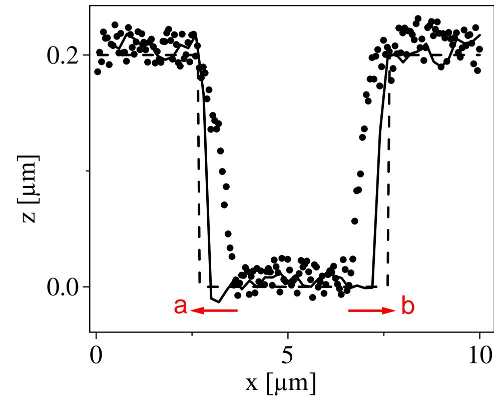

Fig. 3. Topography profile of one hole of the etalon recorded by the setup of Fig. 1 in AFM mode: solid line – profile recorded with sharp etched tip, dots – profile recorded with spherical grinded tip, dash line – nominal rectangular profile of the hole. The arrows a and b indicate the wings of the profile used for tip shape reconstruction.

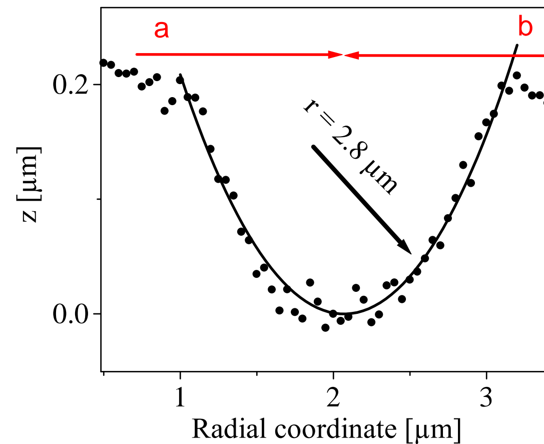

Fig. 4. Restored tip shape after deconvolution: dots - experimental data, solid line – fit with the model of a spherical tip shape, r - the best fitting parameter of the tip curvature radius. The arrows a and b indicate the wings of th e profile of Fig. 3 used for tip shape reconstruction.

For measurement of the near- and far-field light distribution, we coupled a cw He-Ne laser into the fiber and scanned a commercial pin hole of wave-length-range size (diameter 1 µm) with a sensitive photodiode behind it

layer-by-layer at the different distances between tip and pinhole plane (see inset in Fig. 1). A typical intensity distribution of a grinded spherical tip approached to the pinhole plane is shown in Fig. 5. The arrows and the dashed circle indicate the beam diameter (FWHM).

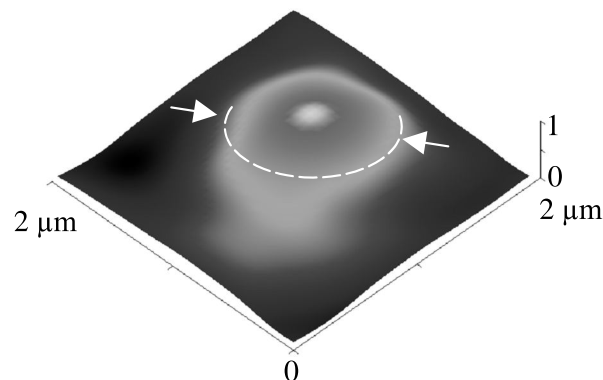

Fig. 5. Intensity map of a grinded spherical tip approached to the pinhole plane. The arrows and circle show the beam diameter.

Fig. 6 shows the dependences of the beam diameter (FWHM) vs. the tip-to-pinhole distance for two grinded multimode fibers with spherical end conical tip shapes, respectively, in lateral planes of the distance from the tip ranging from 0.1 to 50 μm. The spherical tip with a radius of 1.5 μm (obtained from deconvolution) shows an effective focusing effect at a distance of a few micrometers that can be approximately associated with a Gaussian beam. The conical shape of the tip produces a beam with properties similar to a diffraction-free Bessel beam [14]. This beam doesn't change significantly the beam diameter at the whole observed distance range. The beam apparently has no focus. In reality, the beam has probably a smeared-out focus with a value of absolute intensity at the beam axis that is lower than that of a Gaussian beam.

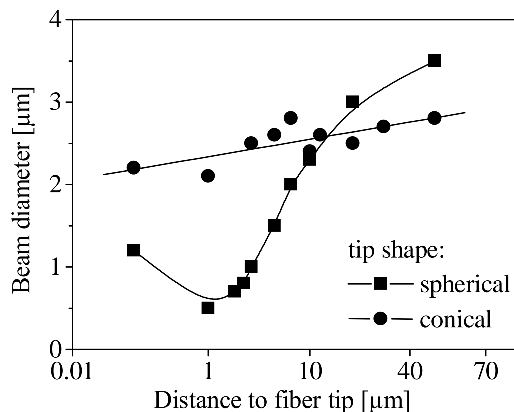

Fig. 6. Comparison of dependence of beam diameter vs. tip-to-pinhole distance for a grinded spherical tip and a grinded conical tip.

We tested a lensed fiber with spherical shape for plasma ignition in a LIBS experiment at an Al surface. At this experiment we used one laser pulse of a coupled-in energy of 25 μJ and a distance of 2 μm between tip and the sample surface. Fig. 7 shows the obtained spectrum from the plasma emission in a wavelength range of 385 to 405 nm. We clearly see the pronounced spectral doublet line of Al. The spectral intensity is considerably higher than that obtained for the same coupled-in pulse energy for a sharp etched fiber, probably due to higher transmission of the fiber tip.

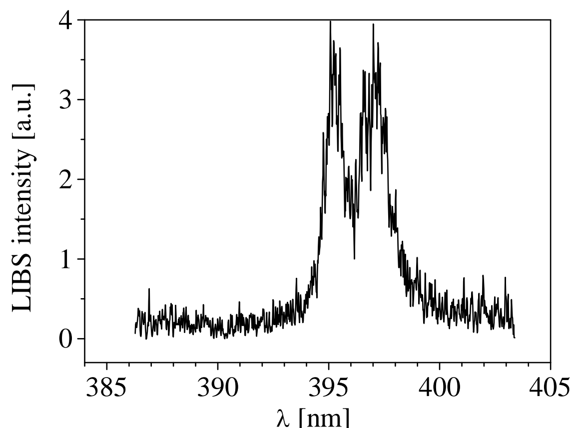

Fig. 7. LIBS spectrum of an Al surface irradiated through a grinded spherical lensed fiber tip with a single 532 nm Nd:YAG laser pulse ($E = 25\ \mu J$). The distance between tip and sample is 2 μm.

4. Conclusions

We combine laser processing and the technique of a scanning near-field optical microscope (SNOM) for laser-patterning on a submicron scale and micro-analysis of solid surface samples by laser-induced breakdown spectroscopy (LIBS). We describe a universal SNOM-like setup allowing to produce patterns by laser ablation, laser-induced plasma ignition, and atomic force microscope (AFM) topography investigation with the same optical fiber tip, which is used as light emitter or as probe. The use of micro-grinded lensed fibers for delivery of the laser light combines the advantages of high numerical aperture optics with high transmission for ns laser pulses. This allows to ignite a plasma for LIBS spectra at a certain distance between sample surface and fiber tip for increased tip durability. The tip quality can be characterized in-situ by deconvolution from AFM topography of etalon grids or by a scanned pinhole for measurement of the near- and far-field light intensity distribution. For grinded spherical tips with radii of a few μm, we see effective focusing that can be approximately associated with a Gaussian beam, while for grinded conical shape of the tip, we produce a beam with properties similar to a diffraction-free Bessel beam. In LIBS experiments, the application of spherical lensed fibers showed an improvement of the LIBS signal compared to the use of sharp etched tips.

Acknowledgements

The Austrian Science Fund FWF under contract P17360-N08, the Austrian NANO Initiative in the project NSI_NBPF, and the Christian Doppler Research Society are acknowledged for financial support. S.Y. wants to thank D. Brodoceanu and M.-A. Bodea for productive discussions.

References

[1] D. Bauerle, Laser Processing and Chemistry, Springer, Berlin, Heidelberg, New York, 3rd ed., 2000.
[2] G. Wysocki, S. T. Dai, T. Brandstetter, J. Heitz, D. Bauerle, Appl. Phys. Lett. **79,** 159 (2001).
[3] G. Wysocki, J. Heitz, D. Bauerle, Appl. Phys. Lett. **84,** 2025 (2004).
[4] T. Stehrer, J. Heitz, SPIE Proc. **6346,** 634626 (2007).
[5] J. Heitz, S. Yakunin, T. Stehrer, G. Wysocki, D. Bauerle, SPIE Proc. **7131,** 71311W (2009).
[6] P. Hoffmann, B. Dutoit, R. P. Salathe, Ultramicroscopy **61,** 165 (1995).
[7] P. Mühlschlegel, J. Toquant, D. W. Pohl, B. Hecht, Rev. Sci. Instrum. **77,** 016105 (2006).
[8] D. Kossakovski, J. L. Beauchamp, Anal. Chem. **72,** 4731 (2000).
[9] D. J. Hwang, H. Jeon, C. P. Grigoropoulos, Appl. Phys. Lett. **91,** 251118 (2007).
[10] D. J. Hwang, H. Jeon, C. P. Grigoropoulos, J. Yoo, R. E. Russo, J. Appl. Phys. **104,** 013110 (2008).
[11] S. Yakunin, T. Stehrer, J. Heitz, Austrian patent Application AT869/2009, 2009.
[12] P. M. Williams, K. M. Shakesheff, M. C. Davies, D. E. Jackson, C. J. Roberts, S. J. B. Tendler, J. Vac. Sci. Technol. **B14,** 1557 (1996).
[13] A. Bukharaev, N. V. Berdunov, D. V. Ovchinnikov, K. M. Salikhov, Scanning Microscopy **12**, 225 (1998).
[14] T. Grosjean, S. S. Saleh, M. A. Suarez, I. A. Ibrahim, V. Piquerey, D. Charraut, P. Sandoz, Appl. Opt. **46,** 8061 (2007).

*Corresponding author: johannes.heitz@jku.at